# Tensor-Based Semi-Blind Receiver for Channel and Symbol Estimation in Frequency-Selective MIMO Systems with Phase Noise Impairments

Paulo R. B. Gomes, Bruno Sokal, and André L. F. de Almeida

***Abstract*— In this paper, we propose a two-stage tensor-based semi-blind receiver for joint channel, phase noise (PN) and symbol estimation for frequency-selective MIMO systems in the presence of PN impairments. In the first stage, the frequency-selective MIMO channel is directly estimated through a tensor-based alternating least squares (ALS) algorithm that fits a PARAFAC model to the noisy received signal. In the second stage, the closed-form least squares Khatri-Rao factorization (LS-KRF) approach is used to extract the PN components at both the transmitter and receiver to be compensated for symbol detection. The proposed receiver has a satisfactory performance compared to the state-of-the-art receivers in terms of symbol error rate (SER). On the other hand, it provides high accuracy individual estimates for the channel and PN, presenting thus a clear advantage over the aforementioned receivers.**

***Keywords*— MIMO systems, joint channel and symbol estimation, PARAFAC decomposition, alternating least squares (ALS), least squares Khatri-Rao factorization (LS-KRF).**

## I. Introduction

Multiple-input multiple-output (MIMO) technologies achieve improved spectral efficiency by employing multiple antennas at both the transmitter and the receiver to exploit the typical array signal processing gains, namely, array diversity, multiplexing and reduced interference gains [1], [2]. However, for the practical implementation of MIMO systems, there are hardware impairments due to non-ideal radio frequency (front-ends), such as oscillator imperfections that result in unknown phase noise (PN) perturbations per antenna. Therefore, distortions can be introduced in the transmitted and received signal leading to a severe performance loss. Moreover, the instantaneous channel acquisition that can be used to improve system performance through precoding/beamforming techniques becomes a challenging problem since the effective channel (PN plus channel) is a distorted version of the true channel, and thus the PN has to be compensated in the channel acquisition step. Therefore, new approaches that can jointly estimate the channel, symbols and PN at the transmitter and receiver have great practical appeal.

The PN compensation in wireless communication systems has been extensively studied in the past years. For instance, in [3] and [4], techniques for PN compensation are proposed for single-input single-output (SISO) systems. However, they assume perfect knowledge of the channel state information (CSI) at the receiver, which is not feasible in practice. Regarding MIMO systems, [5] proposes a novel placement of pilot carriers in the preamble and data portion of the MIMO-OFDM frame for joint channel and PN estimation. The authors in [6], [7] propose compensation schemes based on the knowledge of the statistical modelling of PN process. More recently, [8] presents a pilot signal design scheme for PN mitigation in millimeter wave MIMO-OFDM systems, where the PN plus channel is estimated and compensated for symbol detection. In contrast to works [6], [7], [8], our goal here is to devise a method that can provide individual and accurate channel (instead PN plus channel), symbol and PN estimation by avoiding a prior CSI and PN knowledge and at the same time being robust to PN model variations.

In this paper, we propose a new tensor-based receiver for frequency-selective MIMO systems in the presence of PN impairments. By assuming that each transmitted frame is divided into very small sub-frames and that the PN perturbations are approximately constant over each sub-frame, we show that the received signal can be modeled as a third-order parallel factor (PARAFAC) decomposition [9]. Then, we formulate a two-stage iterative semi-blind receiver for the joint estimation of channel, symbol and PN. In the first stage, estimates of the channel gains are obtained by means of an bilinear ALS algorithm, while the second one obtain closed-form estimates of the PN perturbations per antenna using a LS-KRF approach. The proposed receiver does not require knowledge of the channel and PN model, thus our solution is more realistic compared to other works in the literature that assume a priori knowledge of the CSI and PN process. Simulation results show the effectiveness and high accuracy of the proposed receiver for joint estimation of the channel, symbol and PN.

*Notation:* Scalars are represented as non-bold lower-case letters $a$, column vectors as lower-case boldface letters $\boldsymbol{a}$, matrices as upper-case boldface letters $\boldsymbol{A}$, and tensors as calligraphic upper-case letters $\boldsymbol{\mathcal{A}}$. The superscripts $\{\cdot\}^{\mathrm{T}}$ and $\{\cdot\}^{\dagger}$ stand for transpose and pseudo-inverse operations, respectively. The operator $\|\cdot\|_{\mathrm{F}}$ denotes the Frobenius norm of a matrix or tensor. The operator $\mathrm{diag}\left(\boldsymbol{a}\right)$ converts $\boldsymbol{a}$ into a diagonal matrix, while $D_i\left(\boldsymbol{A}\right)$ forms a diagonal matrix from the $i$-th row of $\boldsymbol{A}$. $\mathrm{vec}\left(\boldsymbol{A}\right)$ converts $\boldsymbol{A} \in \mathbb{C}^{I_1 \times R}$ to a column vector $\boldsymbol{a} \in \mathbb{C}^{I_1 R}$ by stacking its columns on

Paulo R. B. Gomes is with the Federal Institute of Education, Science and Technology of Ceará, Tauá-CE, Brazil. E-mail: paulo.gomes@ifce.edu.br; Bruno Sokal and André L. F. de Almeida are with the Wireless Telecom Research Group (GTEL), Department of Teleinformatics Engineering, Federal University of Ceará, Fortaleza-CE, Brazil. E-mails: {andre,brunosokal}@gtel.ufc.br.

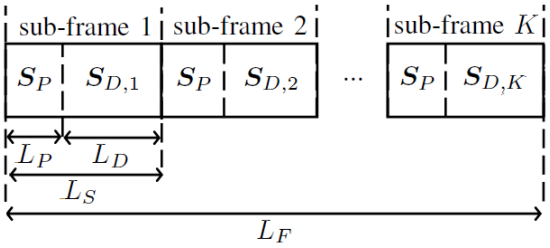


Fig. 1: Illustration of the frame and sub-frame structures.

top of each other. The symbol $\circ$ denotes the outer product operator. $\boldsymbol{A}(i,:) \in \mathbb{C}^{1\times R}$ represents the $i$-th row of $\boldsymbol{A}$. The Khatri-Rao product between $\boldsymbol{A} = [\boldsymbol{a}_1, \ldots, \boldsymbol{a}_R] \in \mathbb{C}^{I_1\times R}$ and $\boldsymbol{B} = [\boldsymbol{b}_1, \ldots, \boldsymbol{b}_R] \in \mathbb{C}^{I_2\times R}$, simbolized by $\diamond$, is defined as

$$\boldsymbol{A} \diamond \boldsymbol{B} = [\boldsymbol{a}_1 \otimes \boldsymbol{b}_1, \boldsymbol{a}_2 \otimes \boldsymbol{b}_2, \ldots, \boldsymbol{a}_R \otimes \boldsymbol{b}_R] \in \mathbb{C}^{I_1 I_2 \times R}. \quad (1)$$

Throughout this paper, we shall make use of the following properties:

$$\text{vec}\left(\boldsymbol{ABC}\right) = \left(\boldsymbol{C}^{\text{T}} \otimes \boldsymbol{A}\right) \text{vec}\left(\boldsymbol{B}\right), \quad (2)$$

$$\text{diag}\left(\boldsymbol{a}\right) \boldsymbol{b} = \text{diag}\left(\boldsymbol{b}\right) \boldsymbol{a}, \quad (3)$$

$$\boldsymbol{a} \otimes \boldsymbol{b} = \text{vec}\left(\boldsymbol{b} \circ \boldsymbol{a}\right), \quad (4)$$

where the vectors and matrices involved have compatible dimensions in each case.

## II. System Model

Let us consider a point to point frequency-selective MIMO system with transmitter and receiver having $M$ and $N$ antennas, respectively. Each transmit and receive antenna is equipped with its own independent oscillator so that the PN is assumed to be different between the antennas. Each transmitted frame of length $L_F = K \cdot L_S$ is composed by $K$ sub-frames, each having length $L_S$. Each sub-frame consists of a known pilot symbols part $\boldsymbol{S}_P \in \mathbb{C}^{M\times L_P}$ of length $L_P$ and an unknown data part $\boldsymbol{S}_{D,k} \in \mathbb{C}^{M\times L_D}$ of length $L_D$. Thus, each transmitted sub-frame has size $L_S = L_P + L_D$. The pilot symbols are reused sub-frame to sub-frame. Figure 1 illustrates the considered frame and sub-frame structures. We assume that the system operates with high sampling rate and the PN is approximately constant[1] within a very small sub-frame, but varying from sub-frame to sub-frame. The channel is frequency-selective with $L$ taps assumed to remain constant over the length of one frame, i.e., the channel vary more slowly than the PN process. In the frequency domain, the received signal $\boldsymbol{X}_{k,f} \in \mathbb{C}^{N\times L_S}$ associated with the $k$-th sub-frame at the $f$-th frequency is denoted by

$$\boldsymbol{X}_{k,f} = \boldsymbol{W} D_k\left(\boldsymbol{\Phi}^{[r]}\right) \boldsymbol{H}_f D_k\left(\boldsymbol{\Phi}^{[t]}\right) \boldsymbol{S}_k + \boldsymbol{W}\boldsymbol{V}_{k,f}, \quad (5)$$

where $\boldsymbol{W} \in \mathbb{C}^{N\times N}$ denotes the combining matrix assumed fixed to all sub-frames and frequencies, $\boldsymbol{H}_f \in \mathbb{C}^{N\times M}$ is the MIMO channel matrix associated with the $f$-th frequency, $\boldsymbol{S}_k = [\boldsymbol{S}_P | \boldsymbol{S}_{D,k}] \in \mathbb{C}^{M\times L_S}$ denotes the $k$-th transmitted sub-frame, and $\boldsymbol{V}_{k,f} \in \mathbb{C}^{N\times L_S}$ is the complex additive white Gaussian noise (AWGN) term. In Equation (5), $\boldsymbol{H}_f$ represents the $f$-th frontal slice of the tensor $\boldsymbol{\mathcal{H}} = \tilde{\boldsymbol{\mathcal{H}}} \times_3 \boldsymbol{F}_L \in \mathbb{C}^{N\times M\times F}$ obtained after the multiplication of the channel impulse response tensor $\tilde{\boldsymbol{\mathcal{H}}} \in \mathbb{C}^{N\times M\times L}$ with a DFT matrix $\boldsymbol{F}_L \in \mathbb{C}^{F\times L}$ along the 3-mode. The $n$-th and $m$-th row of the matrices $\boldsymbol{\Phi}^{[r]} \in \mathbb{C}^{K\times N}$ and $\boldsymbol{\Phi}^{[t]} \in \mathbb{C}^{K\times M}$ are given by

$$\boldsymbol{\Phi}^{[r]}(k,:) = \left[e^{j\theta_1^{[r]}(k)}, \cdots, e^{j\theta_N^{[r]}(k)}\right] \in \mathbb{C}^{1\times N} \quad (6)$$

$$\boldsymbol{\Phi}^{[t]}(k,:) = \left[e^{j\theta_1^{[t]}(k)}, \cdots, e^{j\theta_M^{[t]}(k)}\right] \in \mathbb{C}^{1\times M}. \quad (7)$$

These row vectors contain the unknown PN perturbations $\theta_n^{[r]}(k)$ and $\theta_m^{[t]}(k)$ at the $n$-th $(n = 1, \ldots, N)$ receive antenna and $m$-th $(m = 1, \ldots, M)$ transmit antenna within the $k$-th sub-frame, respectively.

## III. PARAFAC Modeling

At the receiver, the frame shown in Figure 1 is processed in two sequential ways. Firstly, a training-based processing step for joint channel and PN estimation is performed, which is followed by a processing step for PN compensation and symbol detection. In the first step, the receiver extracts only the pilot preamble of each sub-frame. From (5), the pilot contribution $\boldsymbol{X}_{k,f}^{(P)} \in \mathbb{C}^{N\times L_P}$ associated to the $k$-th sub-frame at the $f$-th frequency is represented by

$$\boldsymbol{X}_{k,f}^{(P)} = \boldsymbol{W} D_k\left(\boldsymbol{\Phi}^{[r]}\right) \boldsymbol{H}_f D_k\left(\boldsymbol{\Phi}^{[t]}\right) \boldsymbol{S}_P + \boldsymbol{W}\boldsymbol{V}_{k,f}^{(P)}, \quad (8)$$

where $\boldsymbol{W}\boldsymbol{V}_{k,f}^{(P)} \in \mathbb{C}^{N\times L_P}$ denotes the filtered noise associated to the pilot part of the $k$-th sub-frame. In a similar way, the data contribution $\boldsymbol{X}_{k,f}^{(D)} \in \mathbb{C}^{N\times L_D}$ is given by

$$\boldsymbol{X}_{k,f}^{(D)} = \boldsymbol{W} D_k\left(\boldsymbol{\Phi}^{[r]}\right) \boldsymbol{H}_f D_k\left(\boldsymbol{\Phi}^{[t]}\right) \boldsymbol{S}_{D,k} + \boldsymbol{W}\boldsymbol{V}_{k,f}^{(D)}, \quad (9)$$

where $\boldsymbol{W}\boldsymbol{V}_{k,f}^{(D)} \in \mathbb{C}^{N\times L_D}$ denotes the filtered noise associated to the data symbols of the $k$-th sub-frame. Note that $\boldsymbol{X}_{k,f} = \left[\boldsymbol{X}_{k,f}^{(P)} | \boldsymbol{X}_{k,f}^{(D)}\right] \in \mathbb{C}^{N\times L_S}$.

According the property in Equation (2), by vectorizing $\boldsymbol{X}_{k,f}^{(P)}$ we obtain

$$\boldsymbol{x}_{k,f}^{(P)} = \left(\boldsymbol{S}_P^{\text{T}} \otimes \boldsymbol{W}\right) \text{vec}\left(D_k\left(\boldsymbol{\Phi}^{[r]}\right) \boldsymbol{H}_f D_k\left(\boldsymbol{\Phi}^{[t]}\right)\right) + \tilde{\boldsymbol{v}}_{k,f}^{(P)}, \quad (10)$$

where $\boldsymbol{x}_{k,f}^{(P)} = \text{vec}\left(\boldsymbol{X}_{k,f}^{(P)}\right) \in \mathbb{C}^{NL_P}$ and $\tilde{\boldsymbol{v}}_{k,f}^{(P)} = \text{vec}\left(\boldsymbol{W}\boldsymbol{V}_{k,f}^{(P)}\right) \in \mathbb{C}^{NL_P}$ for simplicity of notation.

By applying again the property in Equation (2) to the second term in the right-hand side of (10), we get

$$\boldsymbol{x}_{k,f}^{(P)} = \left(\boldsymbol{S}_P^{\text{T}} \otimes \boldsymbol{W}\right) \left(D_k\left(\boldsymbol{\Phi}^{[t]}\right) \otimes D_k\left(\boldsymbol{\Phi}^{[r]}\right)\right) \boldsymbol{h}_f + \tilde{\boldsymbol{v}}_{k,f}^{(P)}, \quad (11)$$

where $\boldsymbol{h}_f = \text{vec}\left(\boldsymbol{H}_f\right) \in \mathbb{C}^{NM}$.

Now using the property in Equation (3), we can rewrite (11) as follows

$$\boldsymbol{x}_{k,f}^{(P)} = \left(\boldsymbol{S}_P^{\text{T}} \otimes \boldsymbol{W}\right) \text{diag}\left(\boldsymbol{h}_f\right) \left(\boldsymbol{\Phi}^{[t]\text{T}}(k,:) \otimes \boldsymbol{\Phi}^{[r]\text{T}}(k,:)\right) + \tilde{\boldsymbol{v}}_{k,f}^{(P)}. \quad (12)$$

[1]For most practical oscillators the temporal innovation variance of the PN at each transmit and receive antenna is very small in order of $(10^{-3}, 10^{-5})$ rad$^2$ [10]. Therefore, it is a valid assumption for sub-frames with very small sizes.

Collecting the vectorized received pilots $\boldsymbol{x}_{k,f}^{(P)}$ for all the $k = 1, \ldots, K$ sub-frames that form a given received frame at the $f$-th frequency as the columns of the resulting matrix $\boldsymbol{X}_f^{(P)} = \left[\boldsymbol{x}_{1,f}^{(P)}, \ldots, \boldsymbol{x}_{K,f}^{(P)}\right] \in \mathbb{C}^{NL_P \times K}$, we obtain

$$\boldsymbol{X}_f^{(P)} = \left(\boldsymbol{S}_P^{\mathrm{T}} \otimes \boldsymbol{W}\right) \mathrm{diag}\left(\boldsymbol{h}_f\right) \left(\boldsymbol{\Phi}^{[t]\mathrm{T}} \diamond \boldsymbol{\Phi}^{[r]\mathrm{T}}\right) + \tilde{\boldsymbol{V}}_f^{(P)}, \quad (13)$$

where $\tilde{\boldsymbol{V}}_f^{(P)} = \left[\tilde{\boldsymbol{v}}_{1,f}^{(P)}, \ldots, \tilde{\boldsymbol{v}}_{K,f}^{(P)}\right] \in \mathbb{C}^{NL_P \times K}$.

According to [11], the noiseless term of $\boldsymbol{X}_f^{(P)}$ represents the $f$-th frontal slice of the third-order tensor $\boldsymbol{\mathcal{X}}^{(P)} \in \mathbb{C}^{NL_P \times K \times F}$ which corresponds to the following PARAFAC decomposition

$$\boldsymbol{\mathcal{X}}^{(P)} = \boldsymbol{\mathcal{I}}_{3,MN} \times_1 \left(\boldsymbol{S}_P^{\mathrm{T}} \otimes \boldsymbol{W}\right) \times_2 \left(\boldsymbol{\Phi}^{[t]\mathrm{T}} \diamond \boldsymbol{\Phi}^{[r]\mathrm{T}}\right)^{\mathrm{T}} \times_3 \boldsymbol{H}, \quad (14)$$

where $\boldsymbol{H}(f,:) = \boldsymbol{h}_f^{\mathrm{T}} \in \mathbb{C}^{1 \times MN}$ for $f = 1, \ldots, F$.

The 1-mode, 2-mode and 3-mode unfolding matrices of $\boldsymbol{\mathcal{X}}^{(P)}$ denoted by $\left[\boldsymbol{\mathcal{X}}^{(P)}\right]_{(1)} \in \mathbb{C}^{N_{L_P} \times KF}$, $\left[\boldsymbol{\mathcal{X}}^{(P)}\right]_{(2)} \in \mathbb{C}^{K \times FNL_P}$ and $\left[\boldsymbol{\mathcal{X}}^{(P)}\right]_{(3)} \in \mathbb{C}^{F \times KNL_P}$, respectively, assume the following factorizations with respect to their factor matrices:

$$\begin{aligned}
\left[\boldsymbol{\mathcal{X}}^{(P)}\right]_{(1)} &= \left(\boldsymbol{S}_P^{\mathrm{T}} \otimes \boldsymbol{W}\right) \left(\boldsymbol{H} \diamond \left(\boldsymbol{\Phi}^{[t]\mathrm{T}} \diamond \boldsymbol{\Phi}^{[r]\mathrm{T}}\right)^{\mathrm{T}}\right)^{\mathrm{T}} \\
\left[\boldsymbol{\mathcal{X}}^{(P)}\right]_{(2)} &= \left(\boldsymbol{\Phi}^{[t]\mathrm{T}} \diamond \boldsymbol{\Phi}^{[r]\mathrm{T}}\right)^{\mathrm{T}} \left(\boldsymbol{H} \diamond \left(\boldsymbol{S}_P^{\mathrm{T}} \otimes \boldsymbol{W}\right)\right)^{\mathrm{T}} \\
\left[\boldsymbol{\mathcal{X}}^{(P)}\right]_{(3)} &= \boldsymbol{H} \left(\left(\boldsymbol{\Phi}^{[t]\mathrm{T}} \diamond \boldsymbol{\Phi}^{[r]\mathrm{T}}\right)^{\mathrm{T}} \diamond \left(\boldsymbol{S}_P^{\mathrm{T}} \otimes \boldsymbol{W}\right)\right)^{\mathrm{T}}.
\end{aligned}$$

The above equations are the basis for the formulation of the proposed tensor-based semi-blind receiver that will be presented in the following.

## IV. Proposed Semi-Blind Receiver

Here, our goal is to jointly estimate from the noisy tensor $\boldsymbol{\mathcal{X}}^{(P)}$ in (13) the channel, PN and data symbols without a priori knowledge of the CSI and PN model. The proposed semi-blind receiver consists of two stages. Initially, estimates of $\boldsymbol{H}_f$, for $f = 1, \ldots, F$, are obtained by means of the bilinear ALS (BALS) algorithm [12], [13]. Then, the individual estimates of $\boldsymbol{\Phi}^{[t]}$ and $\boldsymbol{\Phi}^{[r]}$ are obtained by applying the LS-KRF algorithm [14], which are then utilized to compensate the PN during the data symbols detection. In the following, we formulate in detail the steps of the proposed iterative receiver.

### A. *First Stage:* Channel Estimation via BALS

The first stage, called BALS, consists of estimating the factor matrices $\boldsymbol{\Phi} = \left(\boldsymbol{\Phi}^{[t]\mathrm{T}} \diamond \boldsymbol{\Phi}^{[r]\mathrm{T}}\right)^{\mathrm{T}}$ and $\boldsymbol{H}$ in an alternating way from the unfolding matrices $\left[\boldsymbol{\mathcal{X}}^{(P)}\right]_{(2)}$ and $\left[\boldsymbol{\mathcal{X}}^{(P)}\right]_{(3)}$. This can be done by optimizing, respectively, the following two least squares (LS) criteria:

$$\hat{\boldsymbol{\Phi}} = \underset{\boldsymbol{\Phi}}{\mathrm{argmin}} \left\| \left[\boldsymbol{\mathcal{X}}^{(P)}\right]_{(2)} - \boldsymbol{\Phi} \left(\boldsymbol{H} \diamond \left(\boldsymbol{S}_P^{\mathrm{T}} \otimes \boldsymbol{W}\right)\right)^{\mathrm{T}} \right\|_{\mathrm{F}}^2, \quad (15)$$

$$\hat{\boldsymbol{H}} = \underset{\boldsymbol{H}}{\mathrm{argmin}} \left\| \left[\boldsymbol{\mathcal{X}}^{(P)}\right]_{(3)} - \boldsymbol{H} \left(\boldsymbol{\Phi} \diamond \left(\boldsymbol{S}_P^{\mathrm{T}} \otimes \boldsymbol{W}\right)\right)^{\mathrm{T}} \right\|_{\mathrm{F}}^2. \quad (16)$$

The solutions of which are given, respectively, by

$$\hat{\boldsymbol{\Phi}} = \left[\boldsymbol{\mathcal{X}}^{(P)}\right]_{(2)} \left[\left(\boldsymbol{H} \diamond \left(\boldsymbol{S}_P^{\mathrm{T}} \otimes \boldsymbol{W}\right)\right)^{\mathrm{T}}\right]^{\dagger}, \quad (17)$$

$$\hat{\boldsymbol{H}} = \left[\boldsymbol{\mathcal{X}}^{(P)}\right]_{(3)} \left[\left(\boldsymbol{\Phi} \diamond \left(\boldsymbol{S}_P^{\mathrm{T}} \otimes \boldsymbol{W}\right)\right)^{\mathrm{T}}\right]^{\dagger}. \quad (18)$$

Due to the knowledge of $\boldsymbol{W}$ and $\boldsymbol{S}_P$ at the receiver, each iteration of the BALS stage contains only two updating steps. At each step, the fitting error is minimized with respect to one given factor matrix by fixing the other to its value obtained at previous updating step. This procedure is repeated until the convergence of the first stage at the $i$-th iteration. The convergence is declared when $|e_{(i)} - e_{(i-1)}| \leq 10^{-6}$, where $e_{(i)}$ denotes the residual error calculated at the $i$-th iteration defined as $e_{(i)} = \left\| \boldsymbol{\mathcal{X}}^{(P)} - \hat{\boldsymbol{\mathcal{X}}}_{(i)}^{(P)} \right\|_{\mathrm{F}}^2$, where $\hat{\boldsymbol{\mathcal{X}}}_{(i)}^{(P)}$ represents the reconstructed version of $\boldsymbol{\mathcal{X}}^{(P)}$ computed from the estimated factor matrices at the end of the $i$-th iteration.

### B. *Second Stage:* PN Estimation via LS-KRF and Data Symbols Detection

The second stage initially consists of estimating individually each PN matrix $\boldsymbol{\Phi}^{[t]}$ and $\boldsymbol{\Phi}^{[r]}$ by means of the LS-KRF algorithm [14]. Based on the estimated factor matrix $\hat{\boldsymbol{\Phi}}^{\mathrm{T}}$ previously computed in the first stage, let us define $\boldsymbol{\varphi}_k^{[t]} \in \mathbb{C}^M$ and $\boldsymbol{\varphi}_k^{[r]} \in \mathbb{C}^N$ as the $k$-th column of $\boldsymbol{\Phi}^{[t]T}$ and $\boldsymbol{\Phi}^{[r]T}$, respectively. According to definition in Equation (1), we have

$$\hat{\boldsymbol{\Phi}}^{\mathrm{T}} = \left[\boldsymbol{\varphi}_1^{[t]} \otimes \boldsymbol{\varphi}_1^{[r]}, \ldots, \boldsymbol{\varphi}_K^{[t]} \otimes \boldsymbol{\varphi}_K^{[r]}\right] \in \mathbb{C}^{MN \times K}. \quad (19)$$

According to property in Equation (4), the $k$-th column of (19) can be interpreted as the vectorized form of the following rank-1 matrix

$$\boldsymbol{\varphi}_k^{[t]} \otimes \boldsymbol{\varphi}_k^{[r]} = \mathrm{vec}\left(\boldsymbol{\Psi}_k\right), \quad (20)$$

where $\boldsymbol{\Psi}_k = \boldsymbol{\varphi}_k^{[r]} \circ \boldsymbol{\varphi}_k^{[t]} \in \mathbb{C}^{N \times M}$. Therefore, estimates for the vectors $\boldsymbol{\varphi}_k^{[r]}$ and $\boldsymbol{\varphi}_k^{[t]}$ can be obtained by truncating the singular value decomposition (SVD) of $\boldsymbol{\Psi}_k$ defined here as $\boldsymbol{U}_k \boldsymbol{\Sigma}_k \boldsymbol{V}_k^{\mathrm{H}}$ to a rank-1 approximation as follows

$$\hat{\boldsymbol{\varphi}}_k^{[r]} = \sqrt{\sigma_1}\boldsymbol{u}_1 \quad \text{and} \quad \hat{\boldsymbol{\varphi}}_k^{[t]} = \sqrt{\sigma_1}\boldsymbol{v}_1^*, \quad (21)$$

where $\boldsymbol{u}_1 \in \mathbb{C}^N$ and $\boldsymbol{v}_1 \in \mathbb{C}^M$ are the dominant left and right singular vectors of $\boldsymbol{U}_k$ and $\boldsymbol{V}_k$, and $\sigma_1$ is the dominant singular value, respectively. Complete estimates of $\hat{\boldsymbol{\Phi}}^{[r]T}$ and $\hat{\boldsymbol{\Phi}}^{[t]T}$ are obtained repeating the above procedure for $k = 1, \ldots, K$.

At the end, the channel and PN matrices obtained previously can be used to estimate the transmitted data symbols. From (9), by collecting the data symbols part of the $k$-th sub-frame

**Algorithm 1: Proposed Two-Stage Iterative Receiver**

**1. First Stage:** BALS

(1.1) *Set* $i = 0$;
*Initialize randomly the factor matrix* $\hat{\boldsymbol{H}}_{(i=0)}$;

(1.2) $i \leftarrow i + 1$;

(1.3) *According to* (17), *obtain an LS estimate of* $\boldsymbol{\Phi}$:

$$\hat{\boldsymbol{\Phi}}_{(i)} = \left[\boldsymbol{\mathcal{X}}^{(P)}\right]_{(2)} \left[\left(\hat{\boldsymbol{H}}_{(i-1)} \diamond \left(\boldsymbol{S}_P^{\mathrm{T}} \otimes \boldsymbol{W}\right)\right)^{\mathrm{T}}\right]^{\dagger};$$

(1.4) *According to* (18), *obtain an LS estimate of* $\boldsymbol{H}$:

$$\hat{\boldsymbol{H}}_{(i)} = \left[\boldsymbol{\mathcal{X}}^{(P)}\right]_{(3)} \left[\left(\hat{\boldsymbol{\Phi}}_{(i)} \diamond \left(\boldsymbol{S}_P^{\mathrm{T}} \otimes \boldsymbol{W}\right)\right)^{\mathrm{T}}\right]^{\dagger};$$

(1.5) *Repeat steps* (1.2)-(1.4) *until convergence.*

**2. Second Stage:** LS-KRF + Data Symbols Detection

(2.1) *From* $\hat{\boldsymbol{\Phi}}$, *obtained in step (1.3), obtain the estimates of* $\boldsymbol{\Phi}^{[t]}$ *and* $\boldsymbol{\Phi}^{[r]}$ *using the LS-KRF algorithm.*

(2.2) Obtain an LS estimate of $\hat{\boldsymbol{S}}_{D,k}$ according (23);

(2.3) Repeat step (2.2) for $k = 1, \ldots, K$.

for $f = 1, \ldots, F$, we obtain

$$\underbrace{\begin{bmatrix} \boldsymbol{X}_{k,1}^{(D)} \\ \vdots \\ \boldsymbol{X}_{k,F}^{(D)} \end{bmatrix}}_{\boldsymbol{X}_k^{(D)}} = \underbrace{\begin{bmatrix} \boldsymbol{W} D_k\left(\boldsymbol{\Phi}^{[r]}\right) \boldsymbol{H}_1 D_k\left(\boldsymbol{\Phi}^{[t]}\right) \\ \vdots \\ \boldsymbol{W} D_k\left(\boldsymbol{\Phi}^{[r]}\right) \boldsymbol{H}_F D_k\left(\boldsymbol{\Phi}^{[t]}\right) \end{bmatrix}}_{\boldsymbol{H}_k^{(\mathrm{eff})}} \boldsymbol{S}_{D,k} + \underbrace{\begin{bmatrix} \boldsymbol{W}\boldsymbol{V}_{k,1}^{(D)} \\ \vdots \\ \boldsymbol{W}\boldsymbol{V}_{k,F}^{(D)} \end{bmatrix}}_{\tilde{\boldsymbol{V}}_k^{(D)}},$$

or, equivalently,

$$\boldsymbol{X}_k^{(D)} = \boldsymbol{H}_k^{(\mathrm{eff})} \boldsymbol{S}_{D,k} + \tilde{\boldsymbol{V}}_k^{(D)} \in \mathbb{C}^{FN \times L_D}. \tag{22}$$

Therefore, an LS estimation for the data symbols at the $k$-th sub-frame can be obtained from (22) as follows

$$\hat{\boldsymbol{S}}_{D,k} = \left(\hat{\boldsymbol{H}}_k^{(\mathrm{eff})}\right)^{\dagger} \boldsymbol{X}_k^{(D)} \in \mathbb{C}^{M \times L_D}, \tag{23}$$

where

$$\hat{\boldsymbol{H}}_k^{(\mathrm{eff})} = \begin{bmatrix} \boldsymbol{W} D_k\left(\hat{\boldsymbol{\Phi}}^{[r]}\right) \hat{\boldsymbol{H}}_1 D_k\left(\hat{\boldsymbol{\Phi}}^{[t]}\right) \\ \vdots \\ \boldsymbol{W} D_k\left(\hat{\boldsymbol{\Phi}}^{[r]}\right) \hat{\boldsymbol{H}}_F D_k\left(\hat{\boldsymbol{\Phi}}^{[t]}\right) \end{bmatrix} \in \mathbb{C}^{FN \times M} \tag{24}$$

is the effective channel matrix (PN plus channel) constructed from $\hat{\boldsymbol{H}}$, $\hat{\boldsymbol{\Phi}}^{[t]}$ and $\hat{\boldsymbol{\Phi}}^{[r]}$ estimated in the BALS and LS-KRF steps.

The steps of the proposed iterative two-stage tensor-based semi-blind receiver for joint channel, PN and data symbols estimation are summarized in detail in Algorithm 1.

## V. Identifiability Conditions

According to (17) and (18), unique LS solutions for $\boldsymbol{\Phi}$ and $\boldsymbol{H}$ obtained from the unfolding matrices $\left[\boldsymbol{\mathcal{X}}^{(P)}\right]_{(2)}$ and $\left[\boldsymbol{\mathcal{X}}^{(P)}\right]_{(3)}$ requires that $\left(\boldsymbol{H} \diamond \left(\boldsymbol{S}_P^{\mathrm{T}} \otimes \boldsymbol{W}\right)\right)^{\mathrm{T}} \in \mathbb{C}^{MN \times FNL_P}$ and $\left(\boldsymbol{\Phi} \diamond \left(\boldsymbol{S}_P^{\mathrm{T}} \otimes \boldsymbol{W}\right)\right)^{\mathrm{T}} \in \mathbb{C}^{MN \times KNL_P}$ be full row-rank to be right-invertible. Therefore, the following conditions must be satisfied: $FL_P \geq M$ and $KL_P \geq M$. By combining these two conditions, the lower bound on the length of the pilot preamble $L_P$ is given by

$$L_P \geq \max\left(\left\lceil \frac{M}{F} \right\rceil, \left\lceil \frac{M}{K} \right\rceil\right), \tag{25}$$

where $\lceil x \rceil$ denotes the smallest integer number that is greater or equal to $x$.

## VI. Simulation Results

In this section, simulation results are provided to evaluate the performance of the proposed two-stage iterative receiver in terms of the symbol error rate (SER) and the normalized mean equare error (NMSE) of the frequency-selective MIMO channel and PN matrices, which are plotted as a function of the signal-to-noise ratio (SNR). The results represent an average over 1000 Monte Carlo runs. Each run corresponds to and independent realization of the channel, PN, pilots, data symbols, and additive white Gaussian noise (AWGN). The pilot and data symbols are 16-QAM modulated. The PN impairments are modeled as Wiener processes with variance $\sigma^2 = 5 \cdot 10^{-5}$, and independently generated for each transmit and receive antenna. The channel impulse response tensor $\tilde{\boldsymbol{\mathcal{H}}}$ is assumed to have i.i.d complex Gaussian entries with zero-mean and unit variance. The combiner matrix $\boldsymbol{W}$ and $\boldsymbol{F}_L$ are DFT matrices. The remaining system parameters are fixed with the following values: $M = 2$, $N = 2$, $F = 8$ subcarriers and $K = 5$ sub-frames.

Figures 2 and 3 show the NMSE vs. SNR curves of the channel and PN matrices provided by the proposed receiver in **Algorithm 1**, for several values of the pilot size $L_P$. As expected, the estimation accuracy improves when the size of the pilot preambule increases. It is important to note that the proposed receiver provides accurate estimates with very few pilots, thereby corroborating with the assumption of approximately constant PN within very small sub-frames. These two initial experiments demonstrate the effectiveness of the proposed two-stage iterative receiver in estimating jointly the frequency-selective MIMO channel and PN impairments.

Figure 4 compares the SER performance of the proposed method with a LS receiver with and without perfect channel knowledge. In the LS receiver, the effective channel (PN plus channel) is initially estimated from the pilot preamble as $\hat{\boldsymbol{H}}_k^{(\mathrm{eff})} = \boldsymbol{X}_k^{(P)} \boldsymbol{S}_P^{\dagger}$, then the data symbols are obtained according to (23). It can be seen that the LS receiver with perfect channel knowledge outperforms all the other techniques, as expected. We can also observe that the proposed receiver achieves a very close performance, in a low SNR regime, to competitors. However, some performance loss is observed when the SNR increases. This is due to the fact that the proposed receiver make use of the estimated channel and PN matrices (steps 1.3, 1.4 and 2.1 in **Algorithm 1**) in the data symbols detection. Therefore, this performance loss in terms of SER is an impact of the noise estimation in the BALS and LS-KRF stages. On the other hand, as a disadvantage, the

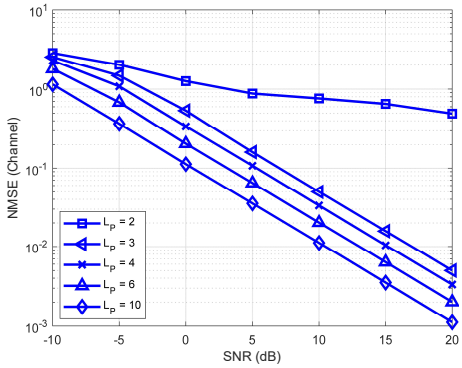


Fig. 2: NMSE of channel vs. SNR performance.

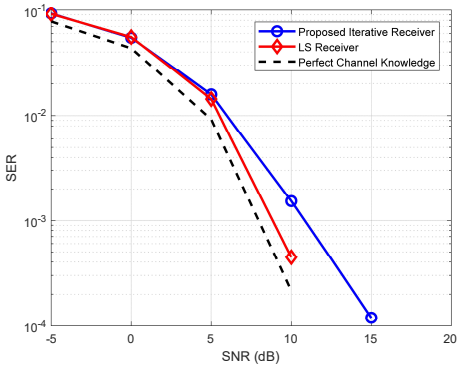


Fig. 4: SER vs. SNR performance.

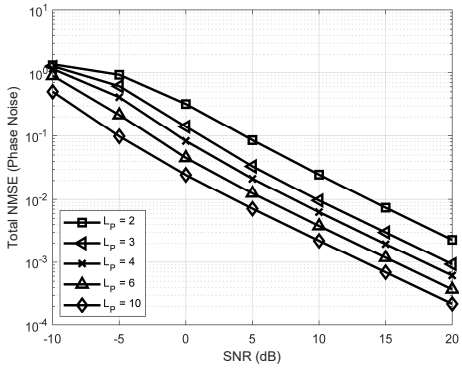


Fig. 3: Total NMSE of PN vs. SNR performance.

LS receiver provides only a distorted estimate of the channel (PN plus channel) instead of the true channel. In contrast, our approach provides accurate estimations closer to the true channel contrarily to the LS receiver, as shown in Figure 2, which can be used for instance to design efficient beamforming strategies in order to achieves better interference rejection, spectral and power efficiency, to exemplify some advantages.

## VII. Conclusion and Perspectives

We have shown that the received signal in a frequency-selective MIMO system with PN impairments can be modeled as a third-order PARAFAC decomposition. Furthermore, we have proposed a two-stage iterative receiver for joint channel, PN and data symbols estimation based on the BALS and LS-KRF algorithms. The proposed approach avoids assumptions such as perfect CSI and PN model knowledge, which makes it applicable to more challenging scenarios compared to other solutions in the literature. Compared to the state-of-the-art LS receiver, our method is able to estimate the data symbols providing also accurate and individual estimates for the PN and true channel (instead PN plus channel), presenting thus a clear advantage over the aforementioned receiver. A perspective of this work is the insertion of channel interpolation in order to decrease the overhead for channel estimation.

## VIII. Acknowledgements

The authors would like to thank to the Coordenação de Aperfeiçoamento de Pessoal de Nível Superior CAPES - Brasil for partially supporting this work (Finance Code 001). The research of André L. F. de Almeida is partially supported by CNPq.

## References

[1] G. J. Foschini, and M. J. Gans, "On limits of wireless communications when using multiple antennas," *Wireless Pers. Commun.*, vol. 6, no. 3, pp. 311-335, 1998.

[2] V. Tarokh, N. Seshadri, and A. R. Calderbank, "Space-time codes for high data rates wireless communications: performance criterion and code construction," *IEEE Trans. Inf. Theory*, vol. 44, no. 2, pp. 744-765, 1998.

[3] D. Petrovic, W. Rave, and G. Fettweis, V. Tarokh, N. Seshadri, and A. R. Calderbank, "Effects of phase noise on OFDM systems with and without PLL: characterization and compensation," *IEEE Trans. Commun.*, vol. 55, pp. 1607-1616, 2007.

[4] K. Y. Kim, Q. Zou, H. J. Choi, and A. H. Sayed, "An efficient carrier phase synchronization technique for high-order M-QAMCOFDM," *IEEE Signal. Process.*, vol. 56, pp. 3789-3794, 2008.

[5] I. M. Ngebani, J. M. Chuma, I. Zibani, E. Matlotse, and K. Tsamaase, "Joint channel and phase noise estimation in MIMO-OFDM systems," *IEEE Radio and Antenna Days of the Indian Ocean*, 2017.

[6] A. Ishaque, and G. Ascheid, "On the efficient mitigation of phase noise in MIMO-OFDM receivers," *International Symposium on Signals, Systems, and Eletronics*, pp. 1-6, Potsdam, Germany, Oct. 2012.

[7] N. Hadaschik, M. Dörpinghaus, A. Senst, U. Käufer, G. Ascheid, and H. Meyer, "Improving MIMO phase noise estimation by exploiting spatial correlations," *IEEE International Conference on Acoustics, Speech, and Signal Processing (ICASSP)*, pp. 833-836, Philadelphia, USA, Mar. 2005.

[8] Y. P. Zhang, J. Liu, S. Feng, and P. Zhang, "Pilot design for phase noise mitigation in millimeter wave MIMO-OFDM systems," *IEEE 85th Vehicular Technology Conference (VTC Spring).*, 2017, pp.1–6.

[9] R. Harshman, "Foundations of the PARAFAC procedure: models and conditions for an explanatory multimodal factor analysis," *UCLA Working Papers in Phonetics*, vol. 16, no. 10, pp. 1-84, 1970.

[10] H. Mehrpouyan, A. A. Nasir, T. Eriksson, S. D. Blostein, G. K. Karagiannidis, and T. Svensson, "Time-varying phase noise and channel estimation in MIMO systems," *IEEE International Workshop on Signal Processing Advances in Wireless Communications (SPAWC)*, Cesme, Turkey, Jun. 2012.

[11] T. G. Kolda, and B. W. Bader, "Tensor decompositions and applications," *Society for Industrial and Applied Mathematics*, vol. 51, no. 3, pp. 455-500, Aug. 2009.

[12] R. Bro, "Multi-way analysis in the food industry: models, algorithms and applications," Ph.D dissertation. University of Amsterdam, Amsterdam, 1998.

[13] A. Smilde, R. Bro, and P. Geladi, *Multi-way analysis*. Wiley, 2004.

[14] F. Roemer and M. Haardt, "Tensor-based channel estimation and iterative refinements for two-way relaying with multiple antennas and spatial reuse," *IEEE Transactions on Signal Processing*, vol. 58, no. 11, pp. 5720-5735, Nov. 2010.